Carbohydrate Polymers 111 (2014) 964–970

Contents lists available at ScienceDirect

Carbohydrate Polymers

journal homepage: www.elsevier.com/locate/carbpol

pH/redox responsive core cross-linked nanoparticles from thiolated carboxymethyl chitosan for in vitro release study of methotrexate

Cheng Gao, Ting Liu, Yinghua Dang, Zhiyan Yu, Wei Wang, Jingjing Guo, Xueqiong Zhang**, Guanghua He, Hua Zheng, Yihua Yin*, Xiangqi Kong

Department of Pharmaceutical Engineering, School of Chemical Engineering, Wuhan University of Technology, Wuhan 430070, PR China

ARTICLE INFO

Article history:
Received 13 February 2014
Received in revised form 3 May 2014
Accepted 6 May 2014
Available online 13 May 2014

Keywords:
Carboxymethyl chitosan
Disulfide
Nanoparticle
pH sensitivity
Reduction responsibility
Controlled drug release

ABSTRACT

A novel amphiphilic thiolated carboxymethyl chitosan was synthesized. It self-assembled into disulfide bond cross-linked nanoparticles in deionized water. The TEM showed that these nanoparticles had a core–shell structure with an average diameter of 160 nm. Dynamic light scattering showed that the nanoparticles were stable in water solution. The particle size changed with pH values and GSH concentrations, and reached a maximum diameter at pH 7.0 and 20 mM GSH respectively, exhibiting an obvious pH/redox responsibility. Methotrexate was encapsulated in nanoparticles reaching encapsulation efficiency as much as 43.4%. Release profiles of methotrexate showed a release rate of 19 wt% in pH 7.4 buffer containing 10 μM GSH, whereas as high as 93 wt% in pH 5.0 buffer containing 20 mM GSH, indicating that the nanoparticles may be used for tumor-specific drug release. The anticancer activity test in vitro showed that the inhibition rate of methotrexate-loaded nanoparticles against HeLa cells reached 90%.

1. Introduction

Over the past decade, controlled drug delivery system has attracted significant attention because it promises to be effective for cancer therapy. Tremendous efforts have been devoted into searching appropriate nano-carriers such as liposomes, micelles and nanoparticles (Peer et al., 2007). Their nano-sized structures are beneficial to the passive targeting of tumor tissue through the enhanced permeability and retention effect (Maeda & Matsumura, 2011). Although considerable work has been done, few of controlled drug delivery systems can achieve the desired outcomes. Their poor stability and inefficient drug release inside the targeted cells are the main challenges.

Various sensitive nanoparticles responding to environment stimulates (pH, temperature, redox potential, and light) have been studied and their intelligent properties may provide a new insight for tumor-targeted and controlled drug delivery. Taking account of slightly acidic environments in cancerous endosomes (pH 5.0–6.5) and lysosomes (pH 4.5–5.0) as compared to those (pH 7.4) in the blood and normal cells (Gerweck & Seetharaman, 1996), the low pH range has been counted as an ideal trigger for the selective release of anti-cancer drugs in cancer cells. So far, many pH responsive nanoparticles have been reported for controlled drug release because they contained reversibly ionizable groups, such as carboxylic or amino groups (Balamuralidhara et al., 2010). To sum up, the pH responsive nanoparticles can be divided into two categories based on the interactions between carrier macromolecules. One kind is formed by weak interactions, such as hydrogen bond interaction and electrostatic interaction, which easily causes serious drug leakage in the circulation of blood due to low stability (Yang et al., 2013). The other is formed by chemical cross-linking with high stability, but leading to limited responsive degree and poor selectivity to tumor cells (Das, Mardyani, Chan, & Kumacheva, 2006).

In view of reports in the literature, the GSH (glutathione) concentrations in the extracellular and intracellular compartments are also distinguished. The disulfide bonds are stable in extracellular fluids (2–20 μM GSH), whereas can reversibly be cleaved in an intracellular reductive environment (2–10 mM GSH). It should further be noted that the concentration of GSH in tumor cells is at least four times higher than that in normal cells (Freya & Garry, 2001). So a great majority of researches have been carried out through the introduction of disulfide-functionalized linkages into nanoparticle carriers for controlled drug release in tumor cells (Aram, Ben, Abhay, & Wang, 2012; Ghazaleh et al., 2013). However, the

* Corresponding author. Tel.: +86 027 87859300; fax: +86 027 87859300.
** Corresponding author.
E-mail addresses: 365464583@qq.com (X. Zhang), yihuayin@aliyun.com (Y. Yin).

http://dx.doi.org/10.1016/j.carbpol.2014.05.012
0144-8617/

concentrations of GSH in normal cells and tumor cells can cleave disulfide bonds in nanoparticles, resulting in poor drug selectivity to tumor cells.

The dual and multi-stimuli responsive nanoparticles could provide a good solution to these issues. They might offer better control over drug delivery and release due to the synergistic effect of multi-stimuli response (Cheng, Meng, Deng, Klok, & Zhong, 2013). At the present time, developing the systems with mild preparation process, uniformity in shape, fine controllable release and simple post-treatment procedure are the goal that researchers are pursuing (Pan et al., 2012).

Chitosan is a naturally occurring polysaccharide consisting of *N*-acetyl glucosamine and glucosamine. However, it is insoluble in the water which greatly limits its application. There are many reports about the modification studies of chitosan (Muzzarelli, Tanfani, Emanuelli, & Mariotti, 1982). Among them, the carboxymethyl chitosan (CM-chitosan), obtained by carboxymethylation reaction of chitosan (Muzzarelli, 1988), has been widely applicated. It retains the advantages of chitosan and has greatly improved water solubility, bioactivity, cell compatibility (Mouryaa, Inamdar, & Tiwari, 2010). In addition, most chemical modifications of chitosan are performed at the free amino groups of the glucosamine units, such as thiolated chitosans constituting an integral part of designated thiomers (Sarti & Bernkop-Schnürch, 2011). The thiolated chitosans have mucoadhesive properties and are used as film agents (Mueller, Verroken, Iqbal, & Bernkop-Schnuerch, 2012). However, the thiolated chitosans are not amphiphilic molecular and difficult to form nanoparticles for drug release in target cells.

Methotrexate (MTX), a stoichiometric inhibitor of dihydrofolate reductase, is extensively for clinical use as an anti-tumor drug. However, its insolubility in water and low bioavailability restricts its clinical application. In addition, its nonspecificity to tumor cell causes side effects such as hair loss, birth defects and a temporary drop in bone marrow function (Yoon et al., 2010).

In this paper, a novel pH/redox sensitive nanoparticle system was prepared by self-assembly of amphiphilic biomacromolecules for improving hydrophobic anticancer drug release in tumor cells. Firstly, CM-chitosan was modified with a hydrophobic thiolated compound, 4-mercaptobenzoic acid (4-MBA) as side chain grafted to the backbone of CM-chitosan. Then, the amphiphilic derivative self-assembled into the nanoparticles through ultrasonic treatment in deionized water. Their structure and morphology were characterized by transmission electron microscope (TEM) and dynamic light scattering (DLS). The stability, pH-sensitivity and reduction responsibility were investigated. In vitro release behavior of MTX-loaded nanoparticles was carried out in pH 7.4 and pH 5.0 media containing various concentrations of GSH. The inhibition activity against HeLa cells was also evaluated.

2. Materials and methods

2.1. Materials

Chitosan with a deacetylation degree of 91% was purchased from the Zhejiang Yuhuan Biotechnology Company, and the MW was 5.6×10^5 Da defined by intrinsic viscosity measurement (Kasaai, Arul, & Charlet, 2000). 4-mercaptobenzoic acid (4-MBA), EDC·HCl and MTX were obtained from Aladdin. 5,5′-Dithiobis(2-nitrobenzoic acid) (DTNB) and GSH were purchased from Biosharp. Dulbecco's modified Eagle's medium (DMEM) was obtained from Gibco. 3-(4,5-dimethylthiazol-2-yl)-2,5-diphenyltetrazolium bromide (MTT) was from Amresco. All other chemicals were of analytical grade.

2.2. Synthesis of CM-chitosan

Chitosan (10 g) was stirred with isopropanol (100 ml) in the three-necked bottle for 6 h and then filtered. The filter residue was alkalizated with 40 ml of NaOH solution (50 wt%), and this solution was fully stirred to mix evenly for 1 h and then frozen in the refrigerator over night. Chloroacetic acid (22 g) dissolved in isopropanol (22 ml) was added dropwise to the alkalizated chitosan and the mixture was stirred for 24 h below 10 °C. This solution was then filtered, and the crude product was purified and finally dried under vacuum. The substitution of carboxymethyl groups was determined by potentiometric titration. The total substitution degree was about 0.66, and the degree of N-substitution was about 0.19.

2.3. Synthesis of thiolated CM-chitosan

4-Mercaptobenzoic acid was coupled to CM-chitosan by the formation of amide linkages through the EDC-mediated reaction. Briefly, 0.1 g CM-chitosan was dissolved in 10 ml deionized water. 4-Mercaptobenzoic acid dissolved in 2 ml of dimethylsulfoxide (DMSO) was activated by EDC·HCl for 2 h (4-MBA/EDC·HCl = 1:1). It was then added dropwise into the CM-chitosan solution and stirred at room temperature in the dark for 6 h. The solution was dialyzed and lyophilized. The whole process was under the protection of nitrogen to minimize oxidation of thiol groups. The pale yellow product was characterized by FT-IR spectroscopy, UV–vis spectroscopy and ^{1}H NMR spectroscopy. The amount of free thiol groups in the product was measured by Ellman's assay (Bernkop-Schnürch, Hornof, & Zoidla, 2003). In the various feed molar ratios of amino groups of CM-chitosan and carboxyl groups of 4-ATP, four samples were synthesized and named as TCM-chitosan-1, TCM-chitosan-2, TCM-chitosan-3 and TCM-chitosan-4, respectively. There about 134.9, 210.4, 285.2 and 360.4 μmol/g thiol moieties were introduced into CM-chitosan, corresponding with approximately 3.1%, 4.8%, 6.5% and 8.2% of polysaccharide units and indicates quantitative substitution of the amino groups with MBA.

2.4. Synthesis of nanoparticles

0.01 g of TCM-chitosan was suspended in 10 ml deionized water and stirred for 1 h at room temperature. Then, the solution was incubated for 6 h in the dark and sonicated by using a probe type sonifier (JY-92IIDN) at 40 W for 3 min to facilitate the oxidation reaction of thiol groups. The resultant solution was filtered through a filter (0.45 μm pore size) to remove dust. Part of resultant solution was freeze-dryed for storage. The nanoparticles prepared from TCM-chitosan-1, TCM-chitosan-2, TCM-chitosan-3 and TCM-chitosan-4 were named NP-1, NP-2, NP-3 and NP-4, respectively. The average particle size and size distribution of the nanoparticles were determined by dynamic light scattering (DLS) with a Zetasizer (Malvern Instruments, Herrenberg, Germany). The measurement was carried out at a detector angle of 90°, a wavelength of 512 nm and a temperature of 25 °C. Morphological evaluation of the nanoparticles was performed by TEM using a Tecnai G2 20 (FEI, USA).

2.5. Stability studies of the nanoparticles

The stability of nanoparticles was studied by placing nanoparticle dispersions at pH 7.4 for a month. Then, the changes of particle sizes and distributions were measured by DLS.

2.6. pH-sensitivity studies of the nanoparticles

0.01 g of nanoparticle dry power was dissolved in PBS of various pH values (3.0, 4.0, 5.0, 6.0, 7.0, 7.4 and 8.0), respectively, and placed in a shaking bed at 200 rpm and 37 °C for 24 h. Then, the particle sizes and distributions of the nanoparticles were determined by DLS. The pH-sensitivity experiments were conducted in triplicate. The results presented are the average data.

2.7. Reduction-response studies of the nanoparticles

The reduction-response studies of the nanoparticles were monitored by DLS measurement. Briefly, the NP-2 dry powers were dissolved in the PBS of pH 7.4 and divided into four parts which were bubbled with N_2 for 10 min in vial. One part was used as control; the other three parts were used for glutathione-response studies by adding GSH to yield different final concentrations of 10 μM, 5 mM and 20 mM, respectively. The three vials were sealed and placed in a shaking bed at 200 rpm and 37 °C for 24 h. The particle sizes and distributions of the nanoparticles were determined by DLS.

2.8. Preparation of MTX-loaded nanoparticles

MTX-loaded nanoparticles were prepared by adding 0.003 M MTX solution in PBS (pH 6.0) to 100 ml of thiolated CM-chitosan solution and then stirring for 1 h followed by sonication for 3 min.

To determine drug-loading efficiency (DLE), 10 ml of MTX-loaded nanoparticle dispersion was centrifuged at high speed of 10,000 rpm for 20 min and the resultant precipitate was freeze-dried for release study. The concentrations of MTX in the decanted aqueous solution were determined by HPLC using a C18 bonded reverse phase column with a mobile phase of V (acetonitrile):V (7.0% citric acid solution):V (2.0% disodium hydrogen phosphate solution) = (10:10:80), at a flow rate of 0.8 ml/min. The peak was detected at 302 nm with a UV detector. The DLE was calculated as follows:

$$\mathrm{DLE}\,(\%) = (W/W_0) \times 100 \quad (1)$$

where W is the mass of drug in nanoparticles and W_0 is the mass of drug-loaded nanoparticles.

The drug-loading efficiency (%) of NP-1, NP-2, NP-3 and NP-4 was 18.5, 43.4, 38.2 and 32.5, respectively.

2.9. Evaluation of in vitro release of MTX-loaded nanoparticles

The release profiles of MTX from nanoparticles were studied in two different buffer solutions (phosphate buffer/pH 7.4; acetate buffer/pH 5.0) with GSH of different concentrations (0, 10 μM, 5 mM, 20 mM). 0.01 g of prepared MTX-loaded NP-2 dry powders were dissolved in 5 ml medium, and immediately transferred to a dialysis bag (molecular weight cut off: 50,000). The dialysis bag was immersed into 35 ml of corresponding medium. The medium was in a thermostatic rotary shaker at speed of 50 rpm at 37 °C. At desired time intervals, 1.0 μL of release medium was taken out for HPLC measurement and replenished with 1.0 μL of fresh medium. The amount of MTX was determined by HPLC using a C18 bonded reverse phase column, with a mobile phase of V (acetonitrile):V (7.0% citric acid solution):V (2.0% disodium hydrogen phosphate solution) = (10:10:80), at a flow rate of 0.8 ml/min. The peak was detected at 302 nm with a UV detector. The cumulative drug release was calculated as follows:

$$\text{Cumulative drug release}(\%) = (M_t/M_0) \times 100 \quad (2)$$

where M_t is the amount of drug released at time t and M_0 is the initial amount of drug in nanoparticles. The release experiments were conducted in triplicate. The results presented are the average data.

2.10. In vitro cytotoxicity measurements

In vitro cytotoxicity was studied by MTT assay using HeLa cells (Wang et al., 2014). The numbers of live cells in the presence of NP-2, free MTX, MTX-loaded NP-2 were counted under the microscope, respectively.

3. Results and discussion

3.1. Synthesis and characterization of CM-chitosan and TCM-chitosan

The schematic syntheses of CM-chitosan and TCM-chitosan were described in Fig. 1(A). Firstly, C_6–OH on chitosan was modified with $ClCH_2COOH$ in alkaline environment to reduce the side reactions on the C3–OH and C2–NH_2, and the water soluble CM-chitosan was obtained. Then, unreacted amino groups of CM-chitosan were modified in subsequent reactions with 4-MBA to yield TCM-chitosan. Since the carboxyl groups also existed in CM-chitosan, the carboxyl groups of 4-MBA was firstly activated with EDC·HCl and the active intermediate ester was obtained. Then the active intermediate ester reacted with C2–NH_2 of CM-chitosan. Thus, it could avoid the activation of the carboxyl groups of CM-chitosan and restrain the side reaction between the carboxyl groups and amino groups of CM-chitosan. In order to protect thiols from cross-linking, the whole reaction process occurred under anaerobic conditions.

UV–vis spectra of CM-chitosan (see curve a) and TCM-chitosan (see curve b) are shown in Fig. 2(A). Compared with curve a, a strong UV absorption band at 254 nm in curve b was observed, which may be attributed to benzene ring of 4-MBA, suggesting that a new substance produced.

The chemical structures of chitosan, CM-chitosan and TCM-chitosan were also determined by IR spectra. In Fig. 2(B), curve a shows the basic characteristics of chitosan at 3455 cm^{-1} (O–H stretch), 2867 cm^{-1} (C–H stretch), 1598 cm^{-1} (N–H bend), 1154 cm^{-1} (bridge-O-stretch), and 1094 cm^{-1}(C–O stretch) (Brugnerotto et al., 2001). Compared with curve a, curve b presented a new characteristic band at 1620 cm^{-1}, which was assigned to carbonyl group (C=O). The other characteristic bands of COOH should be at 3100 cm^{-1} or so, which were covered by O–H hydroxy absorption band. Compared with curve b, a new characteristic band at 2542 cm^{-1} was observed in curve c, which indicated the existence of thiol groups. A new characteristic band at 1490 cm^{-1} was assigned to a stretching vibration of benzene ring, and another obvious characteristic absorption band of the benzene ring should be at 1600 cm^{-1}, which was covered by carbonyl group absorption band. These results showed that 4-MBA was partly linked on CM-chitosan.

The ^1H NMR spectra of CM-chitosan (see curve a) and TCM-chitosan (see curve b) in D_2O are shown in Fig. 2(C). The appearance of the new signals in the region of 7.6–7.8 ppm in curve b was the evidence of benzene ring of 4-MBA. The peak observed at 1.2 ppm corresponded to the chemical shift of –SH group. Thus, the structures of CM-chitosan and TCM-chitosan can be further validated by ^1H NMR spectra.

3.2. Formation and characterization of nanoparticles

A two-step procedure as shown in Fig. 1(B) provides a complete description of the nanoparticle formation process. Firstly, TCM-chitosan self-assembled into nanoparticles with a core–shell

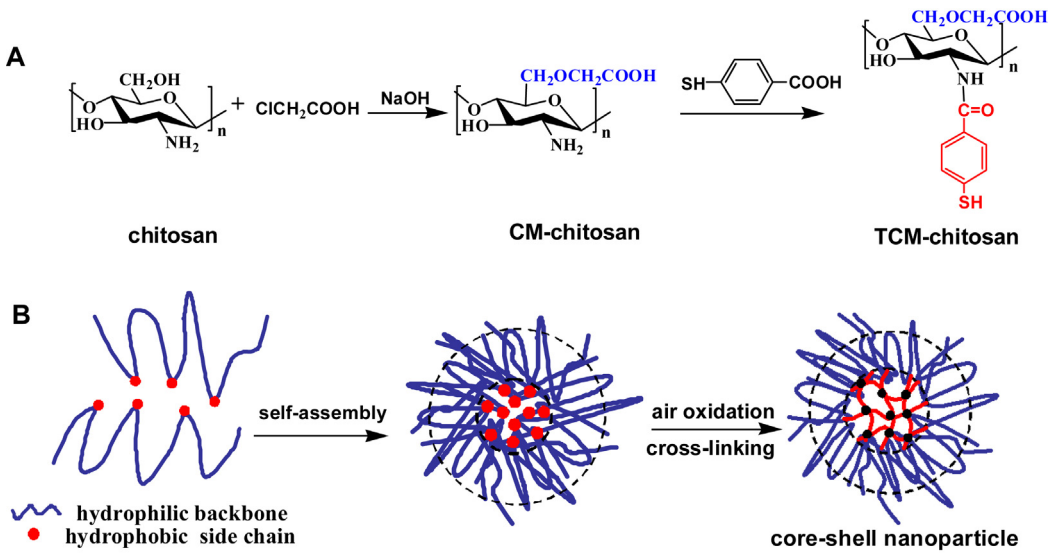

Fig. 1. (A) Synthetic procedure of CM-chitosan and TCM-chitosan; (B) Assembly process of TCM-chitosan.

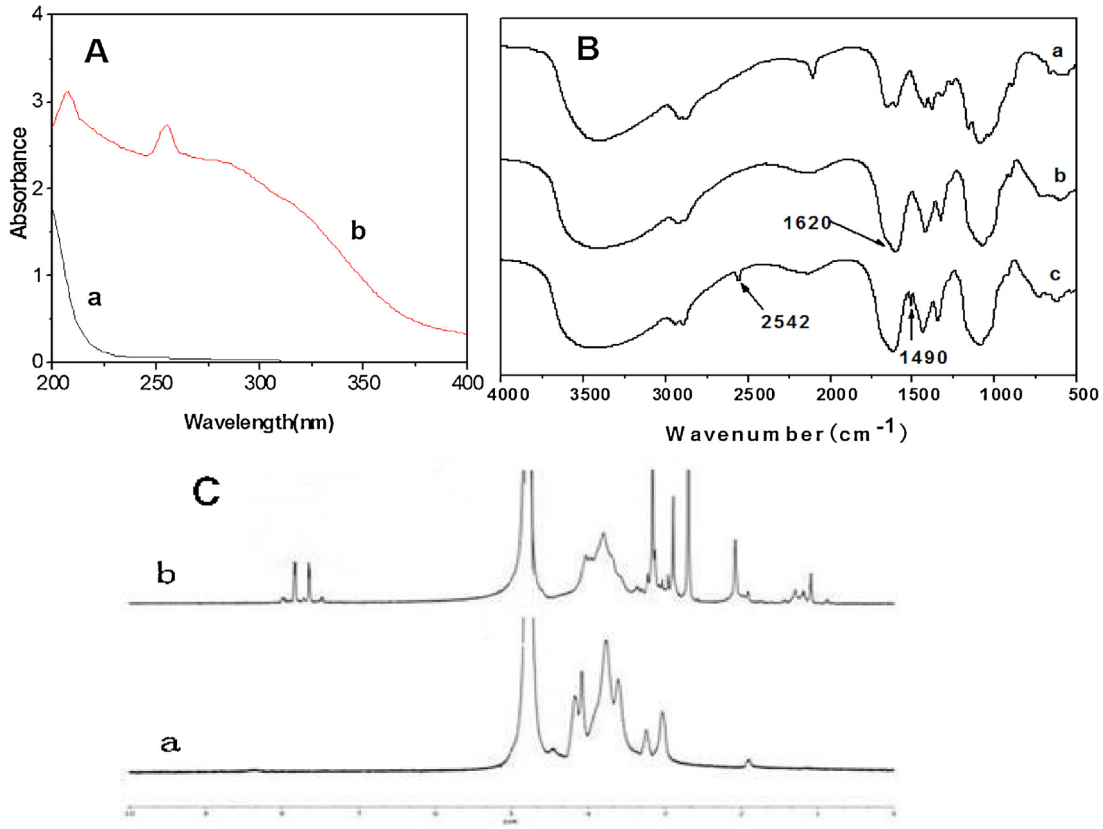

Fig. 2. (A) UV–vis spectra of (a) CM-chitosan and (b) TCM-chitosan; (B) FT-IR spectra of (a) chitosan, (b) CM-chitosan and (c) TCM-chitosan; (C) ^{1}H NMR spectra in D_2O of (a) CM-chitosan and (b) TCM-chitosan.

structure in deionized water. Then, core cross-linked nanoparticles were obtained by air-oxidation under ultrasonication. TEM micrograph in Fig. 3 confirmed the core–shell structure of obtained nanoparticles with a relatively uniform size and a mean value about 160 nm.

TCM-chitosan is an amphiphilic macromolecule consisting of hydrophilic polysaccharide backbone and hydrophobic MBA moieties. In aqueous solution, the hydrophobic chain segments with MBA groups self-aggregated to form a plurality of hydrophobic microdomains, while the hydrophilic segments of carboxymethyl chitosan had a high affinity with water molecules and curled to a hydrophilic shell on the surface of hydrophobic microdomains. Thus, a minimum energy state was maintained stably in solution. At the same time, hydrogen bonds of –COOH groups in curly carboxymethyl chitosan chains made itself shrinked and promoted to wrap the internal hydrophobic microdomains tightly. With the help of ultrasonication, the adjacent thiol groups in the hydrophobic core produced disulfide bonds via air oxidation, and the core

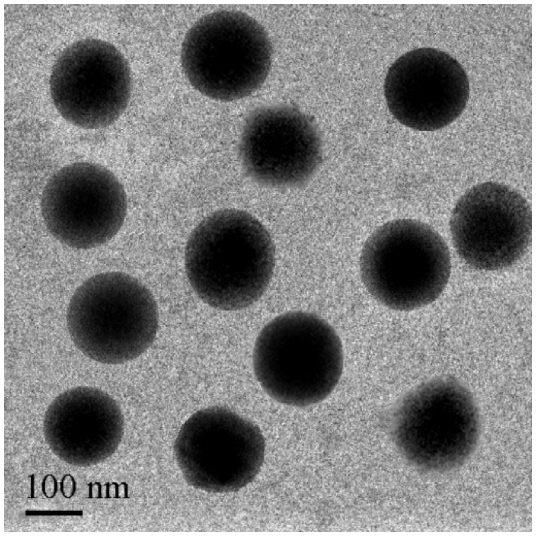

Fig. 3. Representative TEM image of the nanoparticles.

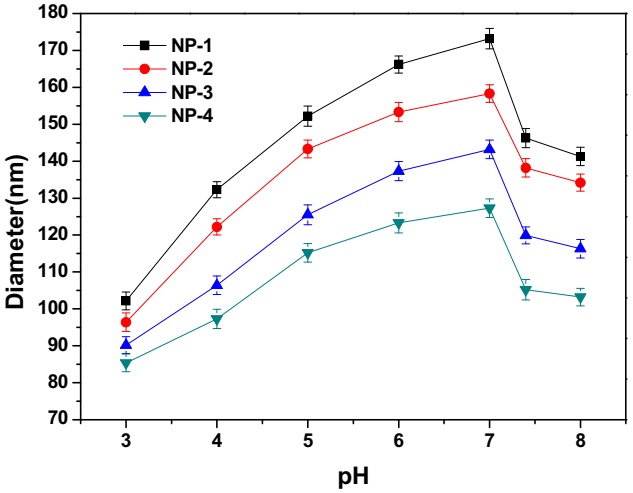

Fig. 4. pH-sensitivity of the nanoparticles.

Table 1
The mean diameters and distributions of nanoparticles at pH 7.4 for their stability.

Sample	Before storage		After storage	
	MD (nm)	PDI	MD (nm)	PDI
NP-1	146	0.055	150	0.063
NP-2	138	0.056	141	0.044
NP-3	119	0.062	120	0.057
NP-4	105	0.047	106	0.051

cross-linked nanoparticles were obtained. The remaining thiol groups in the nanoparticles determined by Ellman's method were less than 10%, which indicated most of thiols were oxidized to form disulfide bonds (García Ruano, Parra, & Alemán, 2008).

3.3. Stability of the nanoparticles

The stability of nanoparticles was studied by determining the changes of mean diameters and distributions of nanoparticles samples stored for 1 month. As shown in Table 1, the mean diameters (MD) and polydispersity index (PDI) values of all samples before and after storage did not change significantly, indicating that the nanoparticles had high stability. This result should be attributed to the core cross-linking of nanoparticles. It is of great significance for avoiding drug leakage before the particles entering the target cells.

3.4. pH-sensitivity of the nanoparticles

The pH-sensitivity of nanoparticles was studied by monitoring the diameter changes of particles at different pH values. As shown in Fig. 4, the diameters of four samples increased when the medium pH was adjusted from 3.0 to 7.0, and all samples had a maximum diameter at pH 7.0. The result could be explained as follows: on the one hand, the ionized extent of carboxyl groups in CM-chitosan was increased from pH 3.0 to 7.0, and a lot of hydrogen bonds between the carboxyl groups were eliminated. On the other hand, the electrostatic repulsion was generated between the ionized carboxyl groups. These two aspects leaded to an increase of the nanoparticle diameters. However, when pH was further increased to 8.0, since the charge screening effect of the counter ions weakened the electrostatic repulsion, a sudden decrease of nanoparticle diameters was observed (Chang et al., 2012; Hua & Wang, 2009). In addition, it was also found that the particle diameters of all samples increased 1.46–1.73 times from pH 3.0 to 7.0 and their change extent was decreased in the following order: NP-1 > NP-2 > NP-3 > NP-4, showing that pH-sensitivity decreased gradually. This result was attributed to a gradual increase of cross-linking degree.

3.5. Reduction-response of the nanoparticles

The reduction-response of nanoparticles was investigated by monitoring the diameter changes of nanoparticles at GSH of different concentrations using DLS. For nanoparticles incubated for 24 h in pH 7.4 buffers with GSH of different concentrations (5 μM, 10 mM and 20 mM), their mean diameters and distributions are shown in Table 2. Compared with the medium without GSH, the particle diameters of four samples almost remained unchanged in the 5 μM GSH buffer; whereas their particle diameters increased obviously in the 5 mM and 20 mM GSH media. Furthermore, the extension of storage time also increased the sample diameters. For example, the particle diameter of NP-2 placed for 3 days at 20 mM GSH was 2.35 times larger than that of NP-2 sample placed for 1 day.

3.6. Loading and release of the nanoparticles

MTX is a hydrophobic drug, which is readily encapsulated in suit into nanoparticles in the process of assembly by mixing with

Table 2
The mean diameters and distributions of nanoparticles at pH 7.4 containing various concentrations of GSH for 24 h.

Sample	GSH (0 μM)		GSH (5 μM)		GSH (5 mM)		GSH (20 mM)	
	MD (nm)	PDI	MD (nm)	PDI	MD (nm)	PDI	MD (nm)	PDI
NP-1	146	0.055	156	0.065	258	0.245	282	0.252
NP-2	138	0.056	144	0.068	236	0.263	262	0.275
NP-3	119	0.062	125	0.055	215	0.261	235	0.278
NP-4	105	0.047	109	0.057	198	0.273	212	0.298

Table 3
The drug loading efficiency of nanoparticles and the solubility of MTX.

Sample	CM-chitosan/4-MBA (mol/mol)	Drug loading efficiency (%)	Solubility (MTX mg/100gH_2O)
NP-1	1/0.6	18.5	25.2
NP-2	1/0.8	43.4	59.1
NP-3	1/1.0	38.2	52.1
NP-4	1/1.2	32.5	44.3

TCM-chitosan solution. Table 3 shows that MTX are efficiently encapsulated into nanoparticles and the drug loading efficiency of NP-2 reaches 43.4%. This may be attributed to the hydrophobic interaction between the nanoparticle core and drug (Torchilin, 2004; Zou, Shi, Wang, & Bo, 2005). Compared with the solubility of free MTX (1 mg/100 g H_2O), a remarkable improvement was observed for that of MTX-loaded NP-2 up to 59.1 mg/100 g H_2O.

Fig. 5 shows the effect of the contents of free thiol groups on the release of the disulfide cross-linked MTX-loaded NPs. As can be seen, the release of the MTX almost stopped after 12 h for all four types of NPs. In pH 7.4 media containing 5 mM GSH, the hydrophilic shell of MTX-loaded NPs swelled and the disulfide bonds in the core were partially split, resulting in a new swelling equilibrium for NPs. Then, the MTX could penetrate the net structure and hydrophilic shell more quickly until reaching a balance concentration inside and outside the NPs. In addition, we found that their cumulative release rates of MTX with time increasing in pH 7.4 media containing 5 mM GSH in the following order: NG-1 > NG-2 > NG-3 > NG-4. This result might be attributed to an increase in cross-linking degree. The nanoparticle with high degree of disulfide cross-linking exhibits small particle size and compact network structure, which would make it more difficult for the MTX release.

As stated in the introduction, the extracellular fluids and normal cells have a 7.4 pH, in which the GSH concentrations are 2–20 μM and 2–10 mM, respectively; while the tumor cells contain slightly acid environment (pH 5.0) and have a higher GSH level (at least 4-fold related to normal cells). Therefore, we chose the following three kinds of media for drug release studies: pH 7.4 medium containing 10 μM GSH, pH 7.4 medium containing 5 mM GSH and pH 5.0 medium containing 20 mM. Fig. 6 shows the drug release behavior from the MTX-loaded NP-2 in the above three media. In pH 7.4 medium containing 10 μM GSH, the release ratio was only about 19 wt%. When the concentration of GSH in the medium increased to 5 mM, the MTX release rate increased to 59 wt%. Whereas in pH 5.0 medium with 20 mM GSH, the MTX release significantly increased

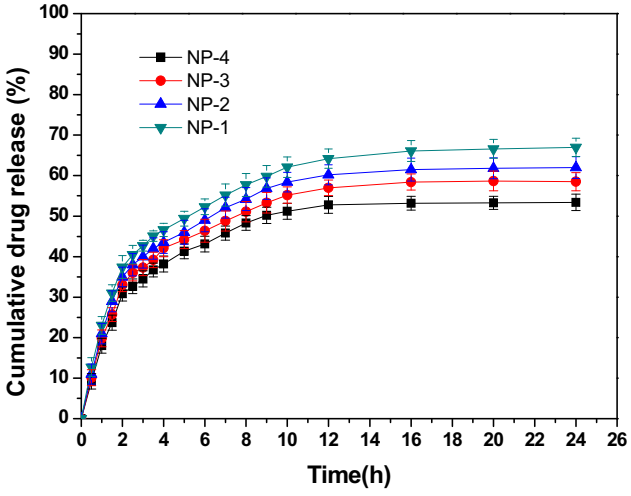

Fig. 5. MTX release profiles from MTX-loaded NPs with various thiol contents in pH 7.4 media containing 5 mM GSH.

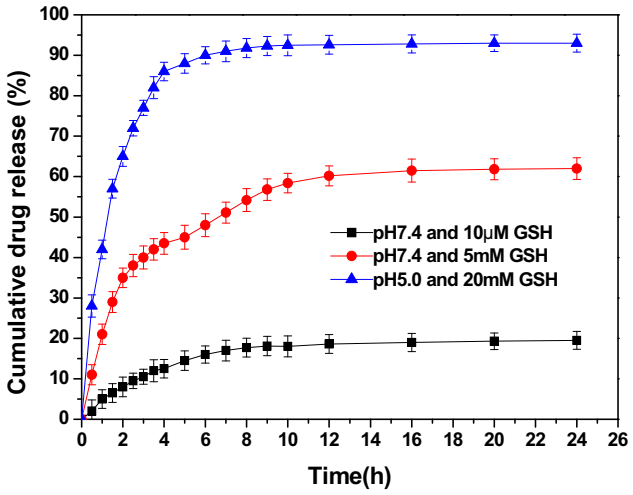

Fig. 6. MTX release profiles from MTX-loaded NP-2 in pH 7.4 media containing 10 μM GSH and 5 mM GSH, and pH 5.0 containing 20 mM GSH.

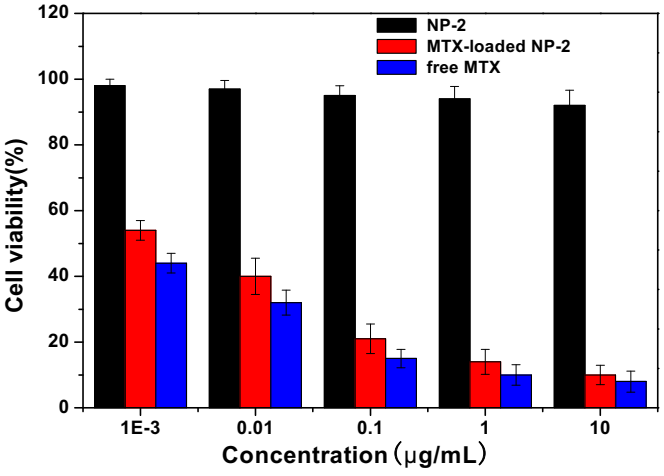

Fig. 7. Viability of HeLa Cells cultured for 48 h with NP-2, free MTX, and MTX-loaded NP-2.

to 93 wt%, suggesting that the MTX-loaded nanoparticles have an excellent controlled release of MTX.

The release mechanism of hydrophobic MTX is based on the diffusion and the degradation of nanoparticles. In pH 7.4 medium containing 10 μM GSH, MTX releases following diffusion mechanism and the swelling degree of nanoparticles acts as the key limiting factor. However, when the concentration of GSH increases to 5 mM, the disulfide bond cleavage is the key limiting factor and the release of MTX is controlled by the degradation mechanism. Whereas in pH 5.0 medium containing 20 mM GSH, the high concentration of GSH splits disulfide bonds and it was the main reason for the fast release of MTX. In addition, we found that the diameter of NP-2 at pH 5.0 was a little larger than that at pH 7.4 in Fig. 4. It meant a larger swelling degree of hydrophilic shell, and it might be an accessory factor in favor of the penetration of external GSH and the exposure of the disulfide bond in cores. These two factors resulted in a rapid and nearly complete release of hydrophobic MTX.

3.7. *In vitro cytotoxicity of MTX-loaded nanoparticles*

To evaluate the effectiveness of nanoparticles as anti-cancer drug carrier for tumor therapy, the in vitro cytotoxicity of MTX-loaded nanoparticles against HeLa cells was investigated. As shown

in Fig. 7, as a control, the NP-2 showed no evident cell cytotoxicity, while a significant cell death was observed when the cells were treated with free MTX and MTX-loaded NP-2, and the cytotoxicity of the MTX-loaded NP-2 was very similar to that of free MTX under the same MTX concentration. This result suggested that the MTX-loaded NP-2 could be efficiently taken up by the HeLa cells and release MTX in response to the intracellular environment.

4. Conclusion

In our study, we synthesized a novel amphiphilic thiolated carboxymethyl chitosan and it self-assembled into core–shell nanoparticles via ultrasonication in deionized water. The shell of nanoparticles containing carboxyl groups could swell in slightly acidic environments and the disulfide bonds in the core could be split by high concentration of GSH. Thus, the pH/redox responsive nanoparticles may be used for tumor-specific drug release. TEM micrographs showed that the nanoparticles had a core–shell structure and a relatively uniform size. No obvious size change was observed by dynamic light scattering for nanoparticles placed for a month in water solution, showed that the nanoparticles had good stability. The profiles of drug release in simulating the in vivo conditions from the MTX-loaded nanoparticles exhibited a selective release in response to the pH and reducing potential in tumor cells and the evaluation of in vitro cytotoxicity showed a remarkable killing effect on HeLa cells, suggesting that the nanoparticle can be utilized as a promising anti-cancer drug carrier for controlled drug release in cancer therapeutics.

Acknowledgements

This research was supported by National Natural Science Foundation of China (No. 51373130, 51273156, 51303145) and the Innovation Research Fund of Wuhan University of Technology (No. 135220001).

References

Aram, O. S., Ben, N., Abhay, P., & Wang, W. X. (2012). The reverse of polymer degradation: In situ crosslinked gel formation through disulfide cleavage. *Chemical Communications*, *48*, 585–587.

Balamuralidhara, V., Pramodkumar, T. M., Srujana, N., Venkatesh, M. P., Vishal, G. N., Krishna, K. L., et al. (2010). pH sensitive drug delivery systems: A review. *American Journal of Drug Discovery and Development*, *1*, 24–48.

Bernkop-Schnürch, A., Hornof, M., & Zoidla, T. (2003). Thiolated polymers-thiomers: Synthesis and in vitro evaluation of chitosan-2-iminothiolane conjugates. *International Journal of Pharmaceutics*, *260*, 229–237.

Brugnerotto, J., Lizardi, J., Goycoolea, F. M., Arguelles-Monal, W., Desbrieres, J., & Rinaudo, M. (2001). An infrared investigation in relation with chitin and chitosan characterization. *Polymer*, *42*, 3569–3580.

Chang, D., Lei, J., Cui, H. R., Lu, N., Sun, Y. J., Zhang, X. H., et al. (2012). Disulfide cross-linked nanospheres from sodium alginate derivative for inflammatory bowel disease: Preparation, characterization, and in vitro drug release behavior. *Carbohydrate Polymers*, *88*, 663–669.

Cheng, R., Meng, F. H., Deng, C., Klok, H. A., & Zhong, Z. Y. (2013). Dual and multi-stimuli responsive polymeric nanoparticles for programmed site-specific drug delivery. *Biomaterials*, *34*, 3647–3657.

Das, M., Mardyani, S., Chan, W. C. W., & Kumacheva, E. (2006). Biofunctionalized pH-responsive microgels for cancer cell targeting: Rational design. *Advanced Materials*, *18*, 80–83.

Freya, Q. S., & Garry, R. (2001). Redox environment of the cell as viewed through the redox state of the glutathione disulfide/glutathione couple. *Free Radical Biology & Medicine*, *30*(11), 1191–1212.

García Ruano, J. L., Parra, A., & Alemán, J. (2008). Efficient synthesis of disulfides by air oxidation of thiols under sonication. *Green Chemistry*, *10*, 706–711.

Gerweck, L. E., & Seetharaman, K. (1996). Cellular pH gradient in tumor versus normal tissue: Potential exploitation for the treatment of cancer. *Cancer Research*, *56*(6), 1194–1198.

Ghazaleh, A., Alireza, S., Shahrouz, T., Mohsen, J., Mohammad, R. K., Mohsen, D., et al. (2013). Synthesis and characterization of thiolated carboxymethyl chitosan-graft-cyclodextrin nanoparticles as a drug delivery vehicle for albendazole. *Journal of Materials Science: Materials in Medicine*, *24*(8), 1939–1949.

Hua, S., & Wang, A. (2009). Synthesis, characterization and swelling behavior of sodium alginate-g-poly (acrylic acid)/sodium humate super absorbent. *Carbohydrate Polymers*, *75*, 79–84.

Kasaai, M. R., Arul, J., & Charlet, G. (2000). Intrinsic viscosity-molecular weight relationship for chitosan. *Journal of Polymer Science Part B-Polymer Physics*, *38*, 2591–2598.

Maeda, H., & Matsumura, Y. (2011). EPR effect based drug design and clinical outlook for enhanced cancer chemotherapy. *Advanced Drug Delivery Reviews*, *63*, 129–130.

Mouryaa, V. K., Inamdar, N. N., & Tiwari, A. (2010). Carboxymethyl chitosan and its applications. *Advanced Materials Letters*, *1*(1), 11–33.

Mueller, C., Verroken, A., Iqbal, J., & Bernkop-Schnuerch, A. (2012). Thiolated chitosans: In vitro comparison of mucoadhesive properties. *Journal of Applied Polymer Science*, *124*(6), 5046–5055.

Muzzarelli, R. A. A. (1988). Carboxymethylated chitins and chitosans. *Carbohydrate Polymers*, *8*(1), 1–21.

Muzzarelli, R. A. A., Tanfani, F., Emanuelli, M., & Mariotti, S. (1982). *N*-Carboxymethylidene chitosans and *N*-carboxymethyl chitosans: Novel chelating polyampholytes obtained from chitosans glyoxylate. *Carbohydrate Research*, *107*, 199–214.

Pan, Y. J., Chen, Y. Y., Wang, D. R., Wei, C., Guo, J., Lu, D. R., et al. (2012). Redox/pH dual stimuli-responsive biodegradable nanohydrogels with varying responses to dithiothreitol and glutathione for controlled drug release. *Biomaterials*, *33*, 6570–6579.

Peer, D., Karp, J. M., Hong, S., Farokhzad, O. C., Margalit, R., & Langer, R. (2007). Nanocarriers as an emerging platform for cancer therapy. *Nature Nanotechnology*, *2*, 751–750.

Sarti, F., & Bernkop-Schnürch, A. (2011). Chitosan and thiolated chitosan. *Chitosan for Biomaterials*, *243*(Part 1), 93–110.

Torchilin, V. P. (2004). Targeted polymeric micelles for delivery of poorly soluble drugs. *Cellular and molecular life sciences*, *61*(19/20), 2549–2559.

Wang, Y. S., Liu, Y., Liu, Y. Y., Wang, Y., Wu, J., Li, R. S., et al. (2014). pH-sensitive pullulan-based nanoparticles for intracellular drug delivery. *Polymer Chemistry*, *5*, 423–432.

Yang, B. H., Li, Y. P., Sun, X. R., Meng, X. L., Chen, P., & Liu, N. (2013). A pH-responsive drug release system based on doxorubicin conjugate-d amphiphilic polymer coated quantum dots for tumor cell targeting and tracking. *Journal of Chemical Technology and Biotechnology*, *88*, 2169–2175.

Yoon, S., Choi, J. R., Kim, J. O., Shin, J. Y., Zhang, X., & Kang, J. H. (2010). Influence of reduced folate carrier and dihydrofolate reductase genes on methotrexate-induced cytotoxicity. *Cancer Research and Treatment*, *42*, 163–171.

Zou, J. H., Shi, W. F., Wang, J., & Bo, J. (2005). Encapsulation and controlled release of a hydrophobic drug using a novel nanoparticle-forming hyperbranched polyester. *Macromolecular Bioscience*, *5*(7), 662–668.